ANTIOXIDANTS & REDOX SIGNALING
Volume 7, Numbers 5 & 6, 2005

Forum Original Research Communication

Energy Status, Ubiquitin Proteasomal Function, and Oxidative Stress During Chronic and Acute Complex I Inhibition with Rotenone in Mesencephalic Cultures

GAIL D. ZEEVALK AND LAURA P. BERNARD

ABSTRACT

Complex I impairment with rotenone produces damage though a mechanism thought to be distinct from effects on mitochondrial respiration. The outcome of chronic rotenone on energy status in relation to toxicity, however, is unknown. To examine this, mesencephalic cultures were exposed to chronic, low-dose rotenone (5–100 n*M*, 8 days *in vitro*) or acute, high-dose rotenone (500 n*M*, 1–24 h), and ATP/ADP levels and toxicity were measured. Chronic exposure to 5–50 n*M* rotenone produced selective dopamine cell loss. High-dose rotenone produced nonselective damage at all exposure times. Chronic, low-dose rotenone (37.5 n*M*) decreased ATP/ADP gradually over several days to 40% of controls, whereas high-dose rotenone (500 n*M*, 1–6 h), collapsed ATP/ADP by 1 h of exposure. The ubiquitin proteasomal pathway, an ATP-dependent pathway, is implicated in Parkinson's disease and, thus, various rotenone exposures were examined for effects on ubiquitin proteasomal function. Chronic, low-dose rotenone (25–50 n*M*, 8 days), but not acute, high-dose rotenone (500 n*M*, 1–6 h), caused accumulation of ubiquitinated proteins, E1-ubiquitin activation, and increased proteasomal activities prior to toxicity even though both exposures increased free radical production. Findings show that selective dopamine cell loss and alterations in ubiquitin proteasomal function only occur with rotenone exposures that partially maintain ATP/ADP. High concentrations of rotenone that collapse energy status kill neurons in a nonselective manner independent of the ubiquitin proteasomal pathway. *Antioxid. Redox Signal.* 7, 662–672.

INTRODUCTION

Loss of nigral dopamine neurons and the presence of Lewy body inclusions characterize Parkinson's disease (PD), the second most common neurodegenerative disease among the elderly population. In familial PD, several genetic mutations have been identified and include mutations in the genes for α-synuclein, parkin, ubiquitin C-terminal hydrolase (33), and DJ-1 (3). Idiopathic PD, on the other hand, does not manifest these genetic mutations, but rather has been associated with biochemical deficits in mitochondrial metabolism involving, by many accounts, complex I (38, 44), but also represented by decreased activities of complex II/III (16), coenzyme Q10 (48), and the Kreb's cycle enzyme α-ketoglutarate dehydrogenase (32). The direct participation of parkin (47) and ubiquitin C-terminal hydrolase (25) in ubiquitin proteasomal function and the accumulation of α-synuclein, as well as the presence of ubiquitin, parkin, and proteasomal subunits in Lewy bodies in both familial and idiopathic PD, strongly implicate the involvement of the ubiquitin proteasomal pathway in both forms of the disease.

1-methyl-4-phenyl-1,2,5,6-tetrahydropyridine (MPTP), a synthetically derived complex I inhibitor, has been used extensively to model idiopathic PD (17, 23) and provide an understanding of the mechanisms associated with dopamine cell damage. Although the acute MPTP model has been informa-

University of Medicine and Dentistry of New Jersey, Robert Wood Johnson Medical School, Department of Neurology, Piscataway, NJ.

tive, it fails, at present, to replicate the accumulation of protein aggregates and inclusion bodies thought to be involved in the disease process. Chronic exposure to low concentrations of the naturally occurring complex I inhibitor rotenone, however, was found *in vivo* in rats to result in ubiquitin-α-synuclein-positive aggregates and loss of nigral dopamine neurons (2). Protein aggregation and dopamine cell damage occurred at estimated brain rotenone levels that, by comparison with isolated brain mitochondria, appeared not to affect mitochondrial respiration (2). *In vitro*, in a neuronal cell line, repeated exposure to 5 n*M* rotenone increased accumulation of α-synuclein (45). In a parallel study from this same report, isolated mitochondria treated with a single application of 5 n*M* rotenone did not show altered NAD-linked O_2 consumption (45). These findings suggest that cell damage caused by the complex I inhibitor rotenone is unrelated to the effects of rotenone on energy production. The relationship of rotenone exposure to energy status and cell damage, however, has not been directly investigated *in situ*.

The following study was carried out to define the energy parameters, ATP, ADP, and ATP/ADP in cells during different rotenone exposures and the relationship to neuronal toxicity. Several steps in the ubiquitin proteasomal pathway are ATP-requiring (5, 19, 52), including the first step in the pathway, *i.e.*, the activation of ubiquitin by E1. The differing effects reported in the literature of acute, high-dose versus chronic, low-dose exposure to complex I inhibitors on protein aggregation could likely be a function of the extent of impairment of high-energy phosphate production during mitochondrial inhibition. To examine this, the effects of different rotenone concentrations and exposures on the ATP-dependent activation of E1 with ubiquitin and accumulation of high-molecular-weight ubiquitinated proteins were also investigated.

MATERIALS AND METHODS

Mesencephalic culture

The ventral mesencephalon from embryonic day 15 rats was dissected, pooled, and mechanically dissociated by trituration. Cells were centrifuged at 1,000 *g* for 10 min and the pellet resuspended in Dulbecco's modified Eagle's medium (DMEM) supplemented with 5 m*M* glucose, 2 m*M* glutamine, and 2.2 g/L bicarbonate plus 10% fetal bovine serum and 10% horse serum (DMEM/serum). Cells were plated at $2.5 \times 10^5/cm^2$ onto a polyornithine-coated substrate in six- or 48-well trays. Cultures were incubated at 37°C in a 95% air/5% CO_2 humidified atmosphere. At 24 h, the culture medium was changed to fresh DMEM/serum. 5-Fluoro-2-deoxyuridine (13 μg) plus uridine (33 μg) was added from days 7–9 *in vitro* to reduce glial growth. The medium was supplemented with 5 m*M* glucose every 72 h until the conclusion of the studies. Rotenone was made as a 10% ethanol stock and diluted to a final ethanol concentration of 0.1%. This concentration of ethanol was found to have no effect on cell viability or the measured outcomes. Rotenone addition was made as indicated for the different experiments. The time of addition of rotenone was such that all exposures were concluded on day 9 *in vitro*. At the end of exposure to rotenone, some cultures were immediately processed for ATP/ADP, proteasomal function, or western blotting as described for the individual procedures. Cultures for toxicity (uptake and immunocytochemistry) had the medium replaced with conditioned DMEM/serum supplemented with 5 m*M* glucose. Conditioned medium was obtained from untreated cultures grown in DMEM/serum for 7–9 days. This has been shown previously to prevent the loss of dopamine neurons caused by refeeding of the culture (9). Cultures for toxicity assessment were returned to the incubator and allowed to recover for 72 h prior to testing to insure that the end points were not a pharmacological effect of treatment, but rather represented irreversible damage.

Dopamine and γ-aminobutyric acid (GABA) high-affinity uptake

The high-affinity uptake of [^{3}H]dopamine (final concentration, 37.5 n*M*) and [^{14}C]GABA (final concentration, 5 μ*M*) was exactly as described previously (10). In brief, cultures were incubated with radiolabeled compounds in HEPES buffer (25 m*M* HEPES, 5.6 m*M* glucose, 125 m*M* NaCl, 4.8 m*M* KCl, 1.2 m*M* KH_2PO_4, 1.3 m*M* $CaCl_2$, 1.2 m*M* $MgSO_4$ containing 1 m*M* ascorbate, 100 μ*M* pargyline, 10 μ*M* aminoxyacetic acid, and 1 m*M* β-alanine for 15 min at 37°C. Radioactivity in the cells was extracted with 95% ethanol and quantified by scintillation counting. Uptake in samples incubated at 4°C was subtracted from other determinations to obtain energy-dependent uptake.

ATP/ADP

ATP and ADP in the cultured cells were measured using the Bioluminescent somatic cell assay kit for ATP from Sigma Chemical Co. (St. Louis, MO, U.S.A.). The chemiluminescence signal was monitored in a luminometer (St. John's Associates, Inc., Beltsville, MD, U.S.A.). ATP was measured according to the manufacturer's protocol supplied with the kit. After reaction and removal of ATP to AMP by luciferen/luciferase, the photometer was rezeroed until a new stable baseline was reached. Phosphoenolpyruvate (final concentration, 0.5 m*M*) plus pyruvate kinase (2 U/assay) was then injected into the assay mix to generate ATP from remaining ADP in the cell lysates. The second increase in chemiluminescence representing ADP was recorded. Quantitation was by comparison with standard curves for ATP and ADP. The standard curve for ADP was generated in the presence of 9.5 μ*M* ATP.

Lactate

The rate of lactate production was measured as described previously (54) following the reduction of NAD spectrophotometrically using lactate dehydrogenase.

Immunocytochemistry and cell counts

Cultures were immunostained for either tyrosine hydroxylase (TH) or neuron-specific enolase (NSE) using a mouse monoclonal anti-TH antibody (1:6,000; Diasorin Inc., Stillwater, MN, U.S.A.) or rabbit polyclonal anti-NSE antibody (undiluted; Oncogene, Cambridge, MA, U.S.A.). The Elite

Avidin, Biotin Peroxidase Vectastain Kit (Vector Laboratories, Burlingame, CA, U.S.A.) and diaminobenzidine were used for visualization. Cell counting was carried out as previously described (55). Counts from 60 1-mm^2 fields from three separate experiments, run in duplicate, were averaged and reported as mean counts per square millimeter ± SEM.

Proteasomal function

Cultured cells were examined for chymotrypsin-like and post acidic-like protease (PAP) activities with modifications to the procedure of Keller *et al.* (21). Cells were lysed in 50 m*M* Tris buffer, 1 m*M* EDTA, pH 7.5, containing 0.1% Triton X-100. The chymotrypsin-like substrate suc-leu-leu-val-tyr-aminomethylcoumarin (AMC) (75 μM) or PAP substrate z-leu-leu-glu-AMC (75 μM) was added to a well, and fluorescence was continuously monitored every 5 min for 1 h at 37°C using 380-nm excitation and 460-nm emission pairing in a Cytofluor 4000 microplate reader (PerSeptive Biosystems, Framingham, MA, U.S.A.). Activity was determined from linear reaction rates and expressed as AMC generated per minute per well. Background was determined in lysates preincubated with the pan-proteasomal inhibitor lactacystin (10 μM). No rate change was observed in the presence of lactacystin, indicating that the increase in fluorescence over time was due to proteasomal cleavage of AMC.

Western blotting

Cells from culture wells were harvested by scraping and placing in buffer containing 10 m*M* HEPES, 2 m*M* EGTA, 2 m*M* EDTA plus 0.2 m*M* phenylmethylsulfonyl fluoride, 25 μl/ml protease inhibitor cocktail mix (Sigma), 1 m*M* dithiothreitol, and 0.1% Triton X-100, pH 7.4. Samples were left on ice for 15 min, sonicated, and the lysates frozen until used for sodium dodecyl sulfate gel separation. Protein [50 μg of whole cell homogenates (ubiquitin) or 50 μg of cell supernatant (E1)] was prepared in sample buffer containing 6 m*M* Tris, 1.7% sodium dodecyl sulfate, 5% glycerol, 0.1 *M* dithiothreitol, and 2% bromophenol blue. Protein samples were loaded onto precast polyacrylamide gels (Bio-Rad, Hercules, CA, U.S.A.) (10–20% discontinuous gel for ubiquitin and 7.5% for E1) and separated by running at 200 V for 55 min. Proteins from the gel were transferred to nitrocellulose using a Panther Semidry Electroblotter (OWL Separation System). The nitrocellulose was exposed to either rabbit polyclonal anti-ubiquitin antibody (1:500; Dako, Carpinteria, CA, U.S.A.) or rabbit polyclonal anti-ubiquitin activating enzyme E1A/E1B antibody (1:2,000; Calbiochem, San Diego, CA, U.S.A.) overnight at 4°C, followed by incubation with the appropriate horseradish peroxidase-conjugated immunoglobulin (Amersham Life Sciences) for 1 h. Visualization was by chemiluminescence using a Western Lightning Kit (PerkinElmer, Life Sciences, Boston, MA, U.S.A.) and exposure to x-ray film.

Reactive oxygen species (ROS) measurement

Cells in culture were loaded with 5 μM dichlorofluorescin diacetate (DCF) (Molecular Probes, Eugene, OR, U.S.A.) for 30 min and washed, and 0.5 ml of HEPES-buffered balanced salt solution (see high-affinity uptake buffer) was added to each well along with various agents to be tested. Fluorescence intensity, (485 nm_{ex}/530 nm_{em}), which is directly proportional to ROS content, was analyzed over the course of 30 min of exposure at 37°C using a CytoFluor multiwell plate reader (Series 4000, PerSeptive Biosystems).

Protein

Protein content for gels was determined using the Bio-Rad reagent. All other protein measurements were determined using the method of Lowry *et al.* (27).

Statistics

Test for significance was carried out by ANOVA with Tukey *post-hoc* treatment. A p value of <0.05 was considered statistically significant.

RESULTS

Selective dopamine cell vulnerability is observed with chronic, low-dose, but not acute, high-dose rotenone exposure

Mesencephalic cultures were exposed to 10–500 n*M* rotenone on days 1–9 *in vitro*. After rotenone removal, cultures were allowed to recover for 3 days and toxicity was assessed. As shown in Fig. 1, low-dose, chronic rotenone exposure produced a selective and dose-dependent toxicity to mesencephalic dopamine neurons at concentrations of rotenone from 10 to 50 n*M*. Consistent with loss of dopamine high-affinity uptake as an index of toxicity, a selective and dose-dependent loss of TH-positive neurons was also observed (Table 1). Toxicity to the other mesencephalic populations as observed by loss of high-affinity GABA transport (Fig. 1) or counts of total neurons (Table 1) was not observed until rotenone exposures reached ≥100 n*M*. At 100 n*M* rotenone, loss of dopamine and GABA uptake was 92.5 and 20%, respectively. At the highest concentration of rotenone tested (500 n*M*, 8 days), there was complete killing of all the cells in the culture. It was found that rotenone from different sources showed different potencies with regard to affects on toxicity and ATP levels. Rotenone from Sigma Chemical Co. was found to be more potent than that from Calbiochem or ICN (data not shown); thus, the same lot of rotenone from Sigma was used for all experiments in this study.

Exposure to 500 n*M* rotenone for 8 days resulted in the complete and nonselective loss of all cells in the culture. It is possible that at shorter times of exposure to a high concentration of rotenone, selective loss of dopamine neurons would be observed. Cultures were, therefore, exposed to 500 n*M* rotenone for various times between 30 min and 24 h, allowed to recover for 3 days, and toxicity was examined (Fig. 2). Toxicity to dopamine and GABA mesencephalic neurons was similar at all times of exposure to high-dose rotenone. Significant toxicity to both the dopamine and GABA population was found beginning with 1 h of exposure and increased with increasing time of exposure. To examine the window of exposure required to produce toxicity to dopamine neurons with

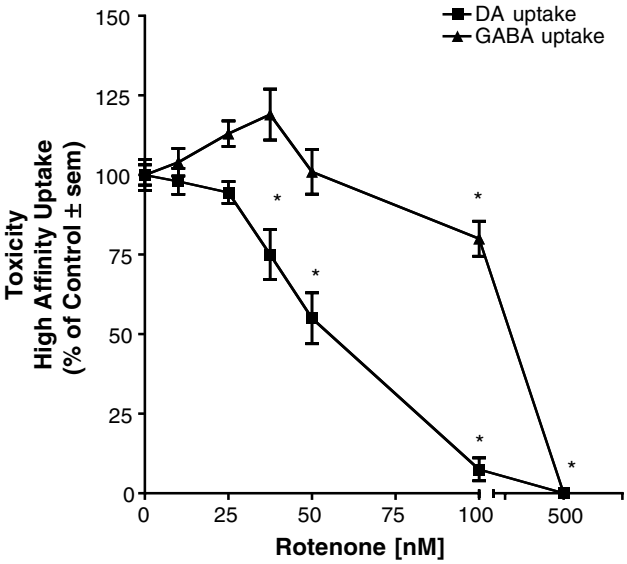

FIG. 1. Dose effects of chronic rotenone on toxicity of mesencephalic dopamine and GABA neurons. Mesencephalic cultures were treated with various concentrations of rotenone for 8 days *in vitro* and allowed to recover 3 days before monitoring of toxicity to the dopamine and GABA neurons as determined by measurement of the high-affinity uptake of ^{3}H-labeled dopamine (DA) and ^{14}C-labeled GABA. Consistent with cell counts (Table 1), selective toxicity to dopamine neurons was observed at the lower concentrations of rotenone. The data are from three or four separate experiments run in duplicate. *Significantly different from zero rotenone.

TABLE 1. TH- AND NSE-POSITIVE CELL COUNTS

Condition	*TH-positive cells/mm² ± SD*	*NSE-positive cells/mm² ± SD*
Control	19.18 ± 2.3	582 ± 54.4
Rotenone		
25 n*M*	17.85 ± 2.5	564 ± 18
37.5 n*M*	15.0 ± 2.3*	593 ± 47.5
50 n*M*	12.1 ± 0.9*	598 ± 107
100 n*M*	2.6 ± 0.6*	458 ± 71*

Exposure to various concentrations of rotenone was carried out in mesencephalic cultures from days 1–9 *in vitro*. Following 3 days of recovery in toxin-free medium, the cultures were examined for TH immunoreactivity. Total neurons in the culture were determined from counts of NSE-positive cells. Cell counting was as described in Materials and Methods. Results are from three separate experiments run in duplicate.

*Different from control.

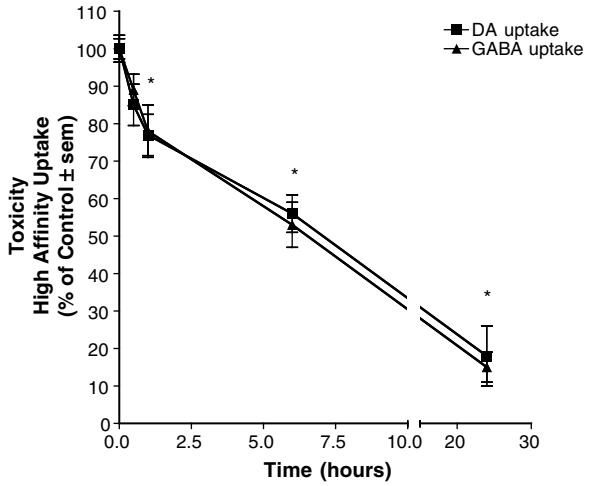

FIG. 2. Effect of time of exposure to high-dose rotenone on mesencephalic dopamine and GABA toxicity. Mesencephalic cultures were treated with 500 n*M* rotenone for 0.5–24 h, then allowed to recover for 3 days before toxicity was determined as described in the legend to Fig. 1. Selective toxicity to mesencephalic dopamine neurons was not observed with exposure to high rotenone concentration. The data are from three experiments run in duplicate. *Significantly different from zero rotenone control.

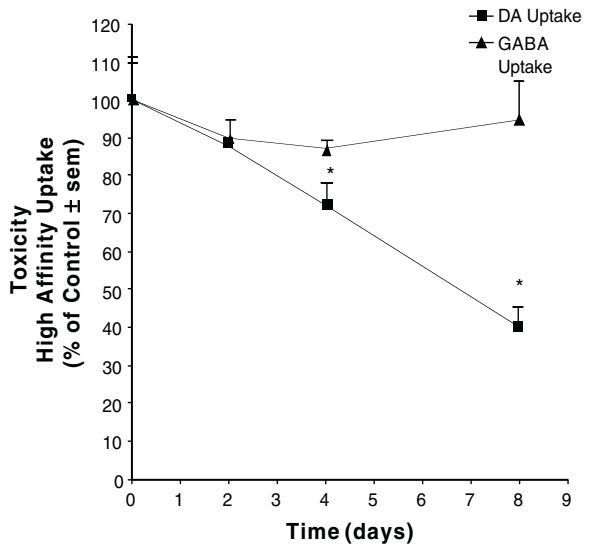

FIG. 3. Effect of time of exposure to low-dose rotenone on mesencephalic dopamine and GABA toxicity. To examine the time window of exposure for toxicity and progression of damage with chronic low-dose rotenone, cultures were exposed to 50 n*M* rotenone for 2, 4, or 8 days *in vitro*, and toxicity was determined following a 3-day recovery period. The data are from three experiments run in duplicate. *Denotes significant difference from zero rotenone cultures.

low-dose, chronic rotenone, cultures were exposed to 50 n*M* rotenone for 2, 4, or 8 days. Exposures were initiated such that all exposures were concluded on day 9 *in vitro*, followed by 3 days of recovery prior to simultaneous measurement of dopamine and GABA high-affinity transport on day 12 *in vitro* (Fig. 3). Exposure to 50 n*M* rotenone for 48 h did not produce toxicity. At 4 and 8 days of exposure, there was progressive toxicity to the dopamine population (28 and 60% loss of dopamine uptake at 4 and 8 days, respectively). Consistent with findings shown in Fig. 1, the GABA population was unaffected by 50 n*M* rotenone.

Energy status during chronic, low-dose and acute, high-dose rotenone

Rotenone has been shown *in vivo* to inhibit complex I nonselectively throughout the brain (2). Our finding of differing effects of chronic, low-dose versus acute, high-dose rotenone exposure on dopamine cell vulnerability, coupled with the nonselective actions of rotenone as a general complex I inhibitor, suggested that the sensitivity of dopamine neurons to rotenone may not be related to its effects on energy metabolism. To examine this, cultures were exposed to either chronic rotenone at a concentration that produced a selective and minimal toxicity to dopamine neurons or to acute high-dose rotenone that produced nonselective damage to all cells, and the effects on ATP and ADP levels were measured following different times of exposure (Table 2). As with the other studies, exposures were initiated such that all exposures were concluded on day 9 *in vitro*. Thus, ATP and ADP values in treated cultures were compared with control cultures at 9 days *in vitro*. Exposure to 37.5 n*M* rotenone for 1, 4, or 8 days produced modest effects on energy status that were maintained over time in culture (Table 2). ATP levels dropped 7, 21, and 24% of control and ADP levels rose 155, 188, and 177% of control at 1, 4, and 8 days of exposure, respectively. The ATP/ADP ratio, which is thermodynamically important in determining the free energy available to drive cellular processes, decreased and was maintained at 41–44% of control. In contrast, 500 n*M* rotenone produced dramatic effects on energy parameters with an ~50% loss of ATP, 6.4-fold increase in ADP, and collapse of the ATP/ADP ratio to <10% of control during 6 h of exposure. Mitochondrial complex I activity could not be directly measured from the primary cultures due to lack of sufficient material for analysis. Therefore, lactate production was used as another approach to monitor the effects of rotenone on aerobic metabolism. The rate of lactate formation was accelerated at all concentrations of rotenone between 5 and 500 n*M* with an increasing rate of production observed with elevating rotenone concentration (Fig. 4). The rate of lactate production in controls was 23 nmol/well/h. These findings indicate that at 5 n*M* rotenone and above there was a partial and incremental inhibition of complex I. Consistent with this, the loss of ATP in cultures incubated with 5–500 n*M* rotenone for 30 min in the absence of glucose was greatly accelerated as compared with ATP loss in the presence of glucose (Fig. 5).

Differing effects of chronic, low-dose and acute, high-dose rotenone on the ubiquitin proteasomal pathway

Both low-dose (37.5 n*M*) and high dose (500 n*M*) rotenone increased ROS production as determined by monitoring DCF fluorescence (Fig. 6), likely leading to oxidative damage. The ubiquitin proteasomal pathway is a major pathway for clearing of oxidatively damaged, short-lived, or misfolded proteins from the cell (6, 15, 42). Several steps in the pathway require ATP. It was, therefore, reasoned that acute, high-dose versus chronic, low-dose rotenone may have different effects on protein ubiquitination and degradation. To examine this, cultures were treated with either 50 n*M* rotenone for 6 h to 8 days *in vitro* or 500 n*M* rotenone for 30 min to 6 h,

Table 2. Effect of Acute and Chronic Rotenone Exposure on Energy Status

	ATP (nmol/mg ± SD)	*ADP (nmol/mg ± SD)*	*ATP/ADP*
Chronic rotenone: days of exposure			
0	23.96 ± 3.59	2.49 ± 0.42	9.70 ± 0.61
1	22.26 ± 2.65	3.86 ± 0.08*	5.80 ± 0.65*
4	18.83 ± 1.86*	4.69 ± 0.30*	4.00 ± 0.47*
8	18.12 ± 2.37*	4.40 ± 0.31*	4.10 ± 0.68*
Acute rotenone: hours of exposure			
0	29.43 ± 4.15	3.56 ± 1.18	8.25 ± 0.49
0.5	22.60 ± 2.98*	8.62 ± 2.80*	2.62 ± 0.60*
1	20.00 ± 0.86*	15.80 ± 4.01*	1.26 ± 0.28*
3	17.90 ± 3.02*	18.62 ± 9.42*	0.96 ± 0.62*
6	15.30 ± 3.53*	22.80 ± 8.64*	0.67 ± 0.42*

Cultures were treated with 37.5 n*M* rotenone for 1, 4, or 8 days or 500 n*M* rotenone for 0.5–6 h *in vitro*. Exposures were initiated so that all exposures were terminated on day 9 *in vitro*. ATP and ADP were measured immediately following exposures using a luciferin/luciferase-generated chemiluminescence as described in Materials and Methods. Data are from three separate experiments for 37.5 n*M* rotenone and four separate experiments for 500 n*M* rotenone, with each parameter run in duplicate.

*Different from 9 days *in vitro* rotenone control.

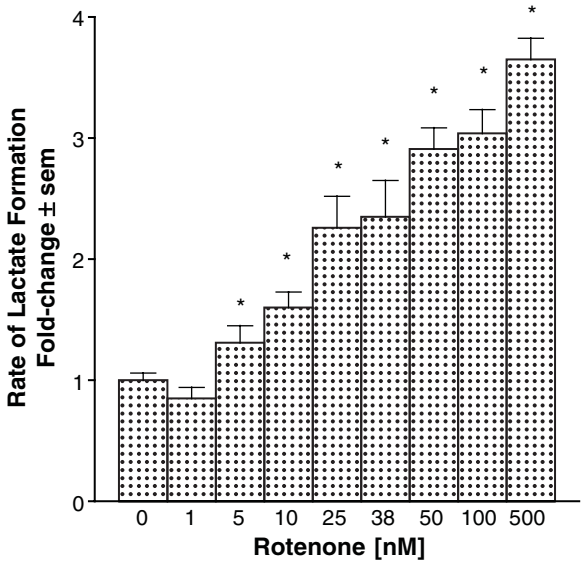

FIG. 4. Rate of lactate production during exposure to various concentrations of rotenone. The rate of lactate formation was determined using an enzyme-based assay as described in Materials and Methods. Lactate levels were determined at 3 and 6 h of exposure to rotenone and calculated as the fold-change in the rate of product formed per hour as compared with controls. The data are from three experiments run in duplicate. *Significantly different from control.

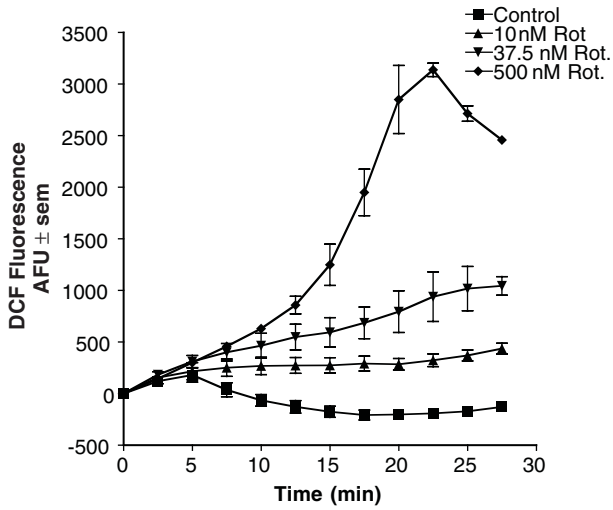

FIG. 6. ROS production during exposure to different concentrations of rotenone. Mesencephalic cultures were treated with various concentrations of rotenone after cells were loaded with the free radical-sensitive probe, DCF (5 μM, 30 min). Free radical generation as monitored by oxidation of the dye was measured every 2.5 min for 30 min using a fluorescent microplate reader as described in Materials and Methods. The data are from three experiments run in duplicate.

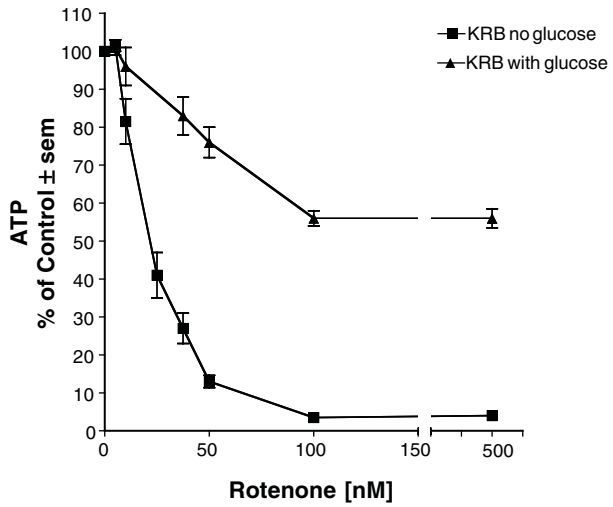

FIG. 5. ATP levels in rotenone treated cultures in the presence or absence of glucose. ATP levels were determined in mesencephalic cultures incubated for 45 min in a bicarbonate-buffered Krebs–Ringer (KRB) with or without 5.5. m*M* glucose. After an initial 15-min preincubation, rotenone was added to the cultures at the indicated concentrations. ATP was measured using a luciferin/luciferase-based assay as described in Materials and Methods. The data are from three determinations run in duplicate.

and levels of high-molecular-weight ubiquitinated proteins and ubiquitin-activating enzyme E1 were examined by western blots. Chronic exposure to 50 n*M* rotenone produced a gradual increase in the accumulation of ubiquitinated proteins by 4 days of exposure (Fig. 7). Total E1 protein (117-kDa band) (Fig. 7) was also found to be elevated at 4 and 8 days of exposure. At these latter time points of rotenone exposure, a second E1-positive band was found at 126 kDa. This upper band could be eliminated by treatment of the sample with β-mercaptoethanol prior to electrophoresis and likely represents the activated E1-ubiquitin complex that is formed by a thiol-ester linkage. Despite the large generation of ROS produced by 500 n*M* rotenone (Fig. 6), acute, high-dose rotenone, in contrast with chronic, low-dose rotenone, neither elevated the accumulation of ubiquitinated proteins nor increased E1 protein or activation (Fig. 8). Because of extensive cell loss at 500 n*M* rotenone, time points longer than 6 h were not followed.

To determine if the buildup of high-molecular-weight ubiquitinated proteins was due to loss of proteasomal activity, proteasomal function was examined by measuring chymotrypsin-like and PAP-like activities in cultures treated with either 37.5 n*M* rotenone for 1, 4, or 8 days or 500 n*M* rotenone for 0.5, 1, 3, or 6 h (Fig. 9). In chronic rotenone-treated cultures, chymotrypsin-like activity was significantly elevated at 1, 4, and 8 days of exposure. PAP activity was also increased with statistical significance observed at 4 days of exposure. In sharp contrast, under conditions of high-dose rotenone, chymotrypsin-like and PAP activities remained unchanged from control at all times of exposure (Fig. 9B).

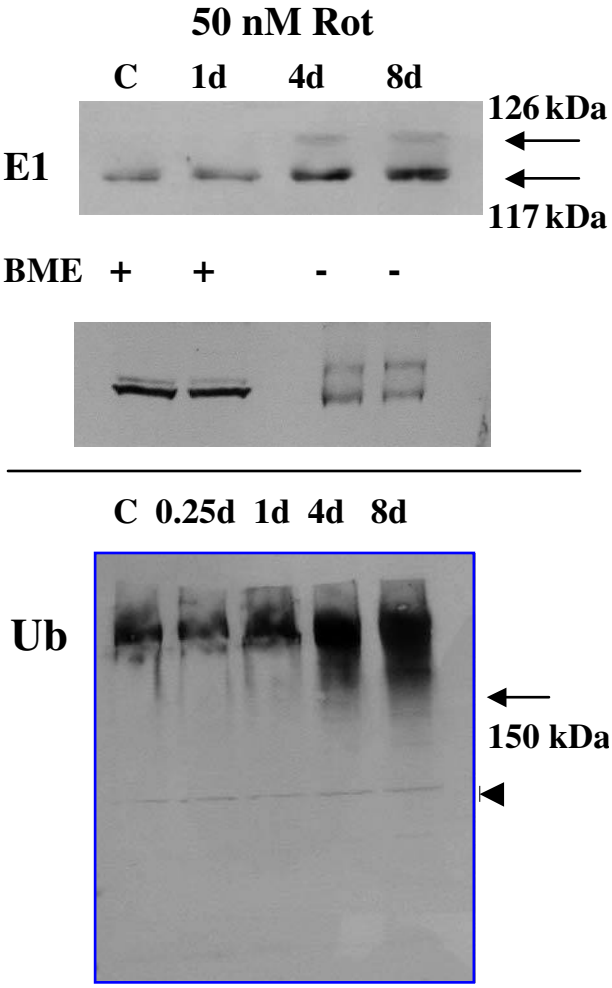

FIG. 7. E1 activation of ubiquitin and accumulation of high-molecular-weight ubiquitinated proteins during chronic exposure to low-dose rotenone. Western blots of E1 protein and high-molecular-weight ubiquitinated (Ub) proteins from cultures treated with 50 n*M* rotenone for various times *in vitro* are presented. Experiments were performed twice with similar results. The intensity of the E1 band at 117 kDa increased with time of rotenone exposure (**top blot**). At 4 and 8 days of rotenone treatment, a second E1-positive band was found at 126 kDa. This band could be eliminated by treatment of the sample with β-mercaptoethanol (BME) prior to running of the gel (**middle blot**). High-molecular-weight ubiquitin-positive proteins increased with increasing time of rotenone exposure (**bottom blot**). Arrowhead denotes a nonspecific band to demonstrate uniformity in loading of the gel.

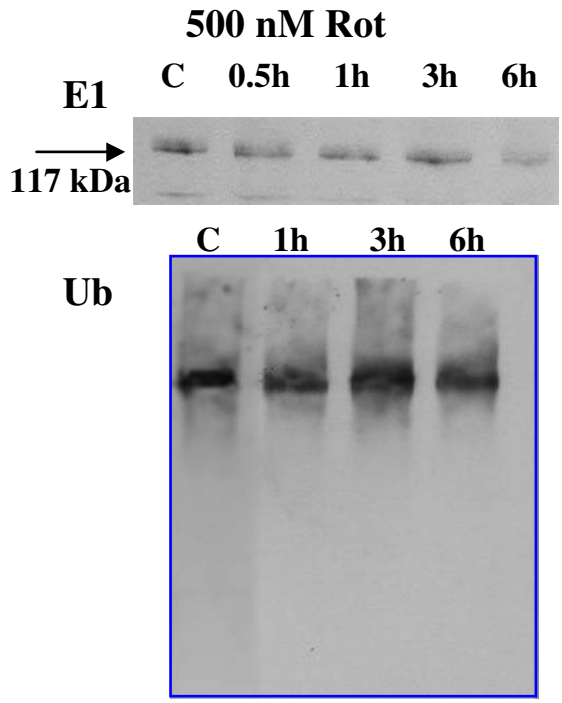

FIG. 8. E1 and ubiquitinated proteins during acute exposure to high-dose rotenone. Western blots of E1 protein and high-molecular-weight ubiquitin (Ub)-reactive proteins from cultures treated with 500 n*M* rotenone for 0.5–6 h are presented. Experiments were performed twice with similar results. Neither E1 protein nor ubiquitinated proteins were found to be increased with exposure to a high concentration of rotenone at times that preceded toxicity.

DISCUSSION

The present study characterized energy status in neurons treated with various concentrations and exposure times of the complex I inhibitor rotenone and determined its relation to ubiquitin proteasomal function and dopamine cell loss. Mitochondrial dysfunction has been identified in idiopathic PD (38, 44). Epidemiological studies suggest that exposure to environmental agents likely plays a role in the etiology of PD (50). Among high-risk factors are exposure to herbicides and pesticides, some of which are mitochondrial poisons (24, 41). Supporting a role for environmentally induced mitochondrial dysfunction in PD were cases of acute-onset parkinsonism caused by exposure to the merperidine analogue MPTP (22). 1-Methyl-4-phenylpyridinium (MPP^+), the toxic metabolite of MPTP, is an inhibitor of complex I (36). Acute exposure to a variety of mitochondrial inhibitors, including MPTP/MPP^+ (12, 23, 28) and rotenone (1, 4, 26), has been shown to produce dopamine cell loss characteristic of PD, but has not replicated the protein aggregation or inclusion body formation that is the histological hallmark of the disease. More recent models of chronic exposure to low concentrations of the complex I inhibitor rotenone *in vivo* (2, 46) and *in vitro* (45) demonstrated toxicity to dopamine neurons or neuroblastoma cells with accompanying accumulation of protein aggregates. Concentrations of rotenone that produced toxicity were speculated to occur independent of effects on mitochondrial respiration. In support of this, rotenone titration in isolated mitochondrial preparations showed little effect on oxygen consumption at rotenone concentrations estimated to be present in brain or cell lines (2, 45). Extrapolation of the effects of a single application of rotenone in isolated mitochondria to whole cells that receive continuous or multiple applications of rotenone is difficult, however, as cumulative effects are not

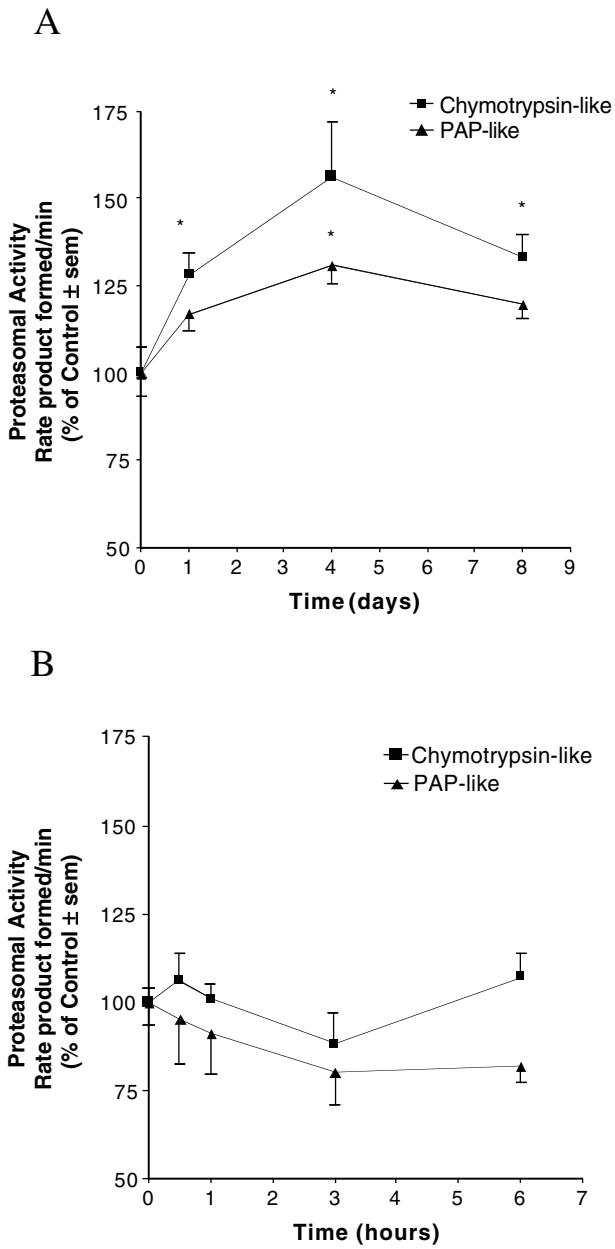

FIG. 9. Proteasomal activity during (A) chronic, low-dose and (B) acute, high-dose exposure to rotenone. Mesencephalic cultures were treated with **(A)** 37.5 n*M* rotenone or **(B)** 500 n*M* rotenone for the indicated times, and proteasomal chymotrypsin-like and PAP-like activities were determined by following the cleavage of an AMC-linked substrate as described in Materials and Methods. The data are from three experiments run in duplicate. *Different from same age cultures that were not exposed to rotenone.

taken into account. This is particularly pertinent to rotenone given its lipophilic nature and slow dissociation rate from complex I. Thus, the issue of ATP/ADP status during rotenone exposure in relation to toxicity and protein aggregation has not been clearly defined, but is important to an understanding of complex I impairment and dopamine cell damage.

The findings show that when ATP/ADP status was maintained at ~40% of basal levels, there was progressive and selective toxicity to mesencephalic dopamine neurons that was preceded by accumulation of high-molecular-weight ubiquitinated proteins and activation of the ubiquitin proteosomal pathway. In contrast, a high concentration of rotenone sharply reduced energy status, killed mesencephalic neurons nonselectively, and did not result in increased levels of ubiquitinated proteins prior to cell death. Both chronic, low-dose and acute, high-dose rotenone exposure resulted in modest to moderate effects on ATP levels (20–25% loss at 4 and 8 days of exposure with 37.5 n*M* rotenone versus 40–48% loss with 500 n*M* rotenone at 3 and 6 h of exposure). ATP levels *per se*, however, are not predictive of the energy available to carry out energy-dependent processes (35). As ATP and ADP approach equilibrium, there is less capacity for energy transfer (35). Thus, with 500 n*M* rotenone exposure, even though ATP levels were somewhat maintained at 3 and 6 h, the drop in energy charge to <10% of basal would not be sufficient to support energy-requiring functions.

One ATP-dependent process relevant to neurodegeneration is the ubiquitin proteasomal pathway, a major pathway for the clearance of damaged proteins from the cell. Ubiquitin-positive protein aggregation has been observed in a number of neurodegenerative diseases (51). Protein ubiquitination and clearance require several ATP-dependent steps, one involving the first step in the pathway, *i.e.*, the activation of ubiquitin by E1 enzyme via the formation of a high-energy thiol ester intermediate (5, 19). The level of energy status maintained with low-dose, chronic rotenone was sufficient to support activation of ubiquitin for subsequent protein conjugation. In contrast, the rapid collapse of ATP/ADP with more complete impairment of mitochondrial respiration by acute, high-dose rotenone inhibited this process from occurring as evidenced by the lack of E1 activation or increase in ubiquitinated proteins.

Selective dopamine cell vulnerability to rotenone has been reported by a number of laboratories (2, 4, 14, 29, 30, 46), but see Hoglinger *et al.* (20). In the current study, however, the selective toxicity of rotenone was only observed with chronic exposures that partially maintained energy status. Although this supports the proposal that the vulnerability of dopamine neurons to chronic rotenone is not related to the effects of rotenone on energy production, it also demonstrates that the selectivity of damage occurs within a narrow range of rotenone concentrations. Thus, this could be a contributing factor for the different findings regarding the selectivity of effects of rotenone found in the literature. One widely held hypothesis for this selective vulnerability is that dopamine neurons are more sensitive to free radical damage promoted by complex I impairment by rotenone. Evidence supports free radical production by rotenone (18, 26) (see Fig. 6) and free radical damage to cells exposed to rotenone (1, 45). Previous work by our laboratory (34) indicates that loss of dopamine homeostasis through impaired vesicular storage and increased cytosolic dopamine contributes to the vulnerability of dopamine neurons during mitochondrial impairment. Cytosolic dopamine unprotected by vesicular sequestration can be oxidized enzymatically or nonenzymatically to produce an oxidative burden that, coupled with ROS production by rotenone, may

overwhelm the cell's antioxidant capacity, leading to degeneration.

The accumulation of high-molecular-weight ubiquitinated proteins during chronic rotenone exposure is consistent with ongoing oxidative damage occurring with rotenone as many oxidatively damaged proteins are targeted by ubiquitination and clearance via the ubiquitin proteasomal pathway (15, 37, 42). Proteasomal activity significantly increased during chronic rotenone exposure. This finding, coupled with the other observed effects on the ubiquitin pathway, suggests a sequela of events during chronic rotenone exposure that includes an increase in oxidatively damaged proteins to trigger increased expression of E1, increased activation of ubiquitin by E1, and an up-regulation of proteasomal activities in an effort to keep pace with damaged proteins. The accumulation of high-molecular-weight ubiquitinated proteins by 4 days of exposure to rotenone, despite the enhancement of ubiquitin proteasomal function, indicates that the production of damaged proteins exceeds the capacity of the cell to remove them. It should be noted that proteasomal activities monitor ATP-independent activity. It is, therefore, possible that *in situ*, ATP levels, although sufficient to maintain E1-ubiquitin activation, are insufficient to supply the 6-ATPases associated with the proteasome that are needed to promote entry of the protein into the core of the proteasome. Also of note is that, although still significantly elevated, the decline in proteasomal activities between 4 and 9 days of rotenone exposure further suggests that ubiquitin-protein accumulation during chronic mitochondrial impairment may ultimately result from an increase in the rate of protein oxidation, as well as a decline in ATP-independent proteasomal activities. A reduction in ATP-independent proteasomal function has been reported in autopsied substantia nigra from PD patients (31). Notably, inhibition of proteasomal function was reported to lead to ubiquitin and α-synuclein labeled inclusions in PC12 cells (40), whereas expression of the A53T mutant α-synuclein in PC12 cells led to loss of proteasomal activity and accumulation of ubiquitinated cytoplasmic aggregates (49). How or if a decline in ATP-dependent or-independent proteasomal function is mechanistically involved in PD is not known at present.

The effects of rotenone on ATP production will be a function of the degree of inhibition of complex I, the threshold effect for inhibition of complex I on respiration (1, 7), and the ability of cells to utilize glucose or aerobically metabolize other substrates to supplement ATP production (1, 26). Neurons cannot produce sufficient ATP solely on the anaerobic metabolism of glucose (53); however, under conditions of enhanced activity (11, 13, 43) or partial deficits in aerobic metabolism (8, 39), anaerobic glycolysis can help to maintain ATP levels. The increase in the rate of lactate production via anaerobic glycolysis has frequently been used to demonstrate an inhibitory effect on aerobic respiration. In the mesencephalic cells, 5–500 n*M* rotenone caused an incremental elevation of lactate production, indicating that rotenone led to a partial and increasing inhibition of complex I. ATP and ADP assessment during short exposures to rotenone in the absence of glucose as compared with its presence supported an inhibitory effect of rotenone on mitochondrial respiration at concentrations that led to selective dopamine cell loss. The selective toxicity to dopamine neurons by rotenone, however, required that the partial inhibition of complex I be carried out under conditions where energy status could be maintained, *i.e.*, in the presence of other metabolizable substrates. In the mesencephalic cultures, the maintenance of ATP levels was supplemented, in part, by the metabolism of glucose to lactate with both high- and low-dose rotenone. As complex I became increasingly impaired, the rate of ATP production was exceeded by its hydrolysis and energy status could not be maintained. In contrast, at low concentrations of rotenone, energy status could be partially sustained to support ATP-dependent processes. Although this served to support the energy needs of the cell and extend cell survival, it also likely contributed to the ongoing oxidative damage to proteins, accumulation of ubiquitinated proteins, and eventual cell loss.

In summary, our findings provide insight into the differing effects of acute versus chronic mitochondrial inhibition on accumulation of high-molecular-weight proteins and neuronal susceptibility. Maintenance of energy status was required for ubiquitin protein accumulation and selective dopamine cell loss during chronic exposure to low concentrations of rotenone, whereas acute, high-dose rotenone did not support protein ubiquitination and resulted in nonselective cell loss. Energy status was partially maintained with low-dose rotenone despite inhibition of mitochondrial respiration. Maintenance of ATP/ADP was achieved by a balance between the degree of inhibition of mitochondrial respiration and the ability of the cell to compensate through metabolism of alternative substrates. Under such conditions, the ubiquitin proteasomal pathway continued to function; however, the capacity to remove damaged proteins was exceeded by the rate of their production. Accumulation of damaged proteins over time could contribute to neuronal dysfunction and cell death. Strategies designed to prevent this may be beneficial in slowing disease progression.

ACKNOWLEDGMENTS

The authors wish to thank Ms. Cindy Song for her skillful technical assistance. This work was supported by a grant from the Parkinson's Disease Foundation and National Institutes of Health grant NS036157.

ABBREVIATIONS

AMC, aminomethylcoumarin; DCF, dichlorofluorescin diacetate; DMEM, Dulbecco's modified Eagle's medium; GABA, γ-aminobutyric acid; MPP^+, 1-methyl-4-phenylpyridinium; MPTP, 1-methyl-4-phenyl-1,2,5,6-tetrahydropyridine; NSE, neuron-specific enolase; PAP, post acidic-like protease; PD, Parkinson's disease; ROS, reactive oxygen species; TH, tyrosine hydroxylase.

REFERENCES

1. Barrientos A and Moraes CT. Titrating the effects of mitochondrial complex I impairment in the cell physiology. *J Biol Chem* 274: 16188–16197, 1999.

2. Betarbet R, Sherer TB, MacKenzie G, Garcia-Osuna M, Panov AV, and Greenamyre JT. Chronic systemic pesticide exposure reproduces features of Parkinson's disease. *Nat Neurosci* 3: 1301–1306, 2000.
3. Bonifati V, Rizzu P, van Baren MJ, Schaap O, Breedveld GJ, Krieger E, Dekker MC, Squitieri F, Ibanez P, Joosse M, van Dongen JW, Vanacore N, van Swieten JC, Brice A, Meco G, van Duijn CM, Oostra BA, and Heutink P. Mutations in the DJ-1 gene associated with autosomal recessive early-onset parkinsonism. *Science* 299: 256–259, 2003.
4. Bywood PT and Johnson SM. Mitochondrial complex inhibitors preferentially damage substantia nigra dopamine neurons in rat brain slices. *Exp Neurol* 179: 47–59, 2002.
5. Ciechanover A, Heller H, Elias S, Haas AL, and Hershko A. ATP-dependent conjugation of reticulocyte proteins with the polypeptide required for protein degradation. *Proc Natl Acad Sci USA* 77: 1365–1368, 1980.
6. Ciechanover A, Finley D, and Varshavsky A. Ubiquitin dependence of selective protein degradation demonstrated in the mammalian cell cycle mutant ts85. *Cell* 37: 57–66, 1984.
7. Davey GP, Peuchen S, and Clark JB. Energy thresholds in brain mitochondria. Potential involvement in neurodegeneration. *J Biol Chem* 273: 12753–12757, 1998.
8. Drewes L, Gilboe DD, and Betz LA. Metabolic alterations in brain during anoxic-anoxia and subsequent recovery. *Arch Neurol* 29: 385–390, 1973.
9. Driscoll BF, Deibler GE, Law MJ, and Crane AM. Damage to neurons in culture following medium change: role of glutamine and extracellular generation of glutamate. *J Neurochem* 61: 1795–1800, 1993.
10. Ehrhart J and Zeevalk GD. Hydrogen peroxide removal and glutathione mixed disulfide formation during metabolic inhibition in mesencephalic cultures. *J Neurochem* 77: 1496–1507, 2001.
11. Fellows LK, Boutelle MG, and Fillenze M. Physiological stimulation increases nonoxidative glucose metabolism in the brain of the freely moving rat. *J Neurochem* 60: 1258–1263, 1993.
12. Forno LS, DeLanney IE, Irwin I, and Langston JW. Electron microscopy of Lewy bodies in the amygdala-parahippocampal region. *Adv Neurol* 69: 217–228, 1996.
13. Fox PT, Raichle ME, Mintun MA, and Dence C. Non-oxidative glucose consumption during focal physiologic neural activity. *Science* 241: 462–464, 1988.
14. Gao H-M, Hong J-S, Zhang W, and Liu B. Distinct role for microglia in rotenone-induced degeneration of dopaminergic neurons. *J Neurosci* 22: 782–790, 2002.
15. Grune T, Reinheckel T, and Davies KJA. Degradation of oxidized proteins in mammalian cells. *FASEB J* 11: 526–534, 1997.
16. Haas RH, Nasirian F, Nakano K, Ward D, Pay RN, Hill R, and Shults CW. Low platelet mitochondrial complex I and complex II/III activity in early untreated Parkinson's disease. *Ann Neurol* 37: 714–722, 1995.
17. Heikkila RE, Hess A, and Duvoisin RC. Dopaminergic neurotoxicity of 1-methyl-4-phenyl-1,2,5,6-tetrahydropyridine in mice. *Science* 224: 1451–1453, 1984.
18. Hensley K, Pye QN, Maidt ML, Stewart CA, Robinson KA, Jaffrey F, and Floyd RA. Interaction of alpha-phenyl-*N-tert*-butyl nitrone and alternative electron acceptors with complex I indicates a substrate reduction site upstream from the rotenone binding site. *J Neurochem* 71: 2549–2557, 1998.
19. Hershko A, Ciechanover A, Heller H, Haas AL, and Rose IA. Proposed role of ATP in protein breakdown: conjugation of proteins with miltiple chains of the polypeptide of ATP-dependent proteolysis. *Proc Natl Acad Sci USA* 77: 1783–1786, 1980.
20. Hoglinger GU, Feger J, Prigent A, Michel PP, Parain K, Champy P, Ruberg M, Oertel WH, and Hirsch EC. Chronic systemic complex I inhibition induces a hypokinetic multisystem degeneration in rats. *J Neurochem* 84: 491–502, 2003.
21. Keller JN, Huang FF, Dimayuga ER, and Maragos WF. Dopamine induces proteasome inhibition in a neuronal PC12 cell line. *Free Radic Biol Med* 29: 1037–1042, 2000.
22. Langston JW, Ballard PA, Tetrud JW, and Irwin I. Chronic parkinsonism in humans due to a product of meperidine analog synthesis. *Science* 219: 979–980, 1983.
23. Langston JW, Forno LS, Rebert CS, and Irwin I. Selective nigral toxicity after systemic administration of 1-methyl-4-phenyl-1,2,5,6-tetrahydropyridine (MPTP) in the squirrel monkey. *Brain Res* 292: 390–394, 1984.
24. LeCouteur DG, McLean AJ, Taylor MC, Woodham BL, and Board PG. Pesticides and Parkinson's disease. *Biomed Pharmacother* 53: 122–130, 1999.
25. Leroy E, Boyer R, Auburger G, Leube B, Ulm G, Mezey E, Harta G, Brownstein M, Jonnalagada S, Chernova T, Dehejia A, Lavedan C, Gasser T, Steinbach P, Wilkinson K, and Polymeropoulos M. The ubiquitin pathway in Parkinson's disease. *Nature* 395: 451–452, 1998.
26. Li N, Ragheb K, Lawler G, Sturgis J, Rajwa B, Melendez JA, and Robinson JP. Mitochondrial complex I inhibitor rotenone induces apoptosis through enhancing mitochondrial reactive oxygen species production. *J Biol Chem* 278: 8516–8525, 2003.
27. Lowry OH, Rosebrough NJ, Farr AL, and Randall RJ. Protein measurement with the Folin phenol reagent. *J Biol Chem* 193: 265–275, 1951.
28. Manaye KF, Sonsalla PK, Barnett G, Heikkila RE, Woodward DJ, Smith WK, and German DC. 1-Methyl-4-(2'-methylphenyl)-1,2,3,6-tetrahydropyridine (2'CH3-MPTP)-induced degeneration of mesostriatal dopaminergic neurons in the mouse: biochemical and neuroanatomical studies. *Brain Res* 491: 307–315, 1989.
29. Marey-Semper I, Gelman M, and Levi-Strauss ML. The high sensitivity to rotenone of striatal dopamine uptake suggests the existence of a constitutive metabolic deficiency in dopaminergic neurons from the substantia nigra. *Eur J Neurosci* 5: 1029–1034, 1993.
30. Marey-Semper I, Gelman M, and Levi-Strauss M. A selective toxicity toward cultured mesencephalic dopaminergic neurons is induced by the synergistic effects of energetic metabolism impairment and NMDA receptor activation. *J Neurosci* 15: 5912–5918, 1995.
31. McNaught KS and Jenner P. Proteasomal function is impaired in substantia nigra in Parkinson's disease. *Neurosci Lett* 297: 191–194, 2001.
32. Mizuno Y, Matsuda S, Yoshino H, Mori H, Hattori N, and Ikebe SI. An immunohistochemical study on αketoglu-

tarate dehydrogenase complex in Parkinson's disease. *Ann Neurol* 35: 204–210, 1994.
33. Mouradain MM. Recent advances in the genetics and pathogenesis of Parkinson disease. *Neurology* 58: 179–185, 2002.
34. Moy LY, Zeevalk GD, and Sonsalla PK. Role for dopamine in malonate-induced damage in vivo in striatum and in vitro in mesencephalic cultures. *J Neurochem* 74: 1656–1665, 2000.
35. Nicholls DG and Ferguson SJ. *Bioenergetics 2*. London and San Diego: Academic Press, 1992.
36. Nicklas WJ, Vyas I, and Heikkila RE. Inhibition of NADH-linked oxidation in brain mitochondria by 1-methyl-4-phenylpyridine, a metabolite of the neurotoxin, 1-methyl-4-phenyl-1,2,5,6-tetrahydropyridine. *Life Sci* 36: 2503–2508, 1985.
37. Pacifici RE, Salo DC, and Davies KJA. Macroxyproteinase (MPO): a 670 kDa proteinase complex that degrades oxidatively denatured proteins in red blood cells. *Free Radic Biol Med* 7: 521–536, 1989.
38. Parker WD, Boyson SJ, and Parks JK. Abnormalities of the electron transport chain in idiopathic Parkinson's disease. *Ann Neurol* 26: 719–733, 1989.
39. Rehncrona S, Rosen I, and Siesjo BK. Brain lactic acidosis and ischemic cell damage. *J Cereb Blood Flow Metab* 1: 297–311, 1981.
40. Rideout HJ, Larsen KE, Sulzer D, and Stefanis L. Proteasomal inhibition leads to formation of ubiquitin/alpha-synuclein-immunoreactive inclusions in PC12 cells. *J Neurochem* 78: 899–908, 2001.
41. Ritz B and Yu F. Parkinson's disease mortality and pesticide exposure in California 1984–1994. *Int J Epidemiol* 29: 323–329, 2000.
42. Salo DC, Pacifici RE, and Davies KJA. Superoxide dismutase undergoes proteolysis and fragmentation following oxidative modification and inactivation. *J Biol Chem* 265: 11919–11927, 1990.
43. Sappey-Marinier D, Calabrese G, Fein G, Hugg JW, Biggins C, and Weiner MW. Effect of photic stimulation on human visual cortex lactate and phosphates using ^{1}H and ^{31}P magnetic resonance spectroscopy. *J Cereb Blood Flow Metab* 12: 584–592, 1992.
44. Schapira AH, Cooper JM, Dexter D, Jenner P, Clark JB, and Marsden CD. Mitochondrial complex I deficiency in Parkinson's disease. *Lancet* 1: 1269, 1989.
45. Sherer TB, Betarbet R, Stout AK, Lund S, Baptista M, Panov AV, Cookson MR, and Greenamyre JT. An in vitro model of Parkinson's disease: linking mitochondrial impairment to altered alpha-synuclein metabolism and oxidative damage. *J Neurosci* 22: 7006–7015, 2002.
46. Sherer TB, Kim J-H, Betarbet R, and Greenamyre JT. Subcutaneous rotenone exposure causes highly selective dopaminergic degeneration and alpha-synuclein aggregation. *Exp Neurol* 179: 9–16, 2003.
47. Shimur H, Hattori N, Kubo S, Mizuno Y, Asakawa S, Minoshima S, Shimizu N, Iwai K, Chiba T, Tanaka K, and Suzuki T. Familial Parkinson disease gene product, parkin, is a ubiquitin-protein ligase. *Nat Genet* 25: 302–305, 2000.
48. Shults CW, Haas RH, Passov D, and Beal MF. Coenzyme Q10 levels correlate with the activities of complexes I and II/III in mitochondria from parkinsonian and nonparkinsonian subjects. *Ann Neurol* 42: 261–264, 1997.
49. Stefanis L, Larsen KE, Rideout HJ, Sulzer D, and Greene LA. Expression of A53T mutant but not wild-type alpha-synuclein in PC12 cells induces alterations of the ubiquitin-dependent degradation system, loss of dopamine release, and autophagic cell death. *J Neurosci* 21: 9549–9560, 2001.
50. Tanner CM, Ottman R, Goldman SM, Ellenberg J, Chan P, Mayeux R, and Langston JW. Parkinson disease in twins: an etiologic study. *JAMA* 281: 341–346, 1999.
51. Trojanowski JQ and Lee VMY. Parkinson's disease and related synucleinopathies are a new class of nervous system amyloidoses. *Neurotoxicology* 23: 457–460, 2002.
52. Varshavsky A. The ubiquitin system. *Trends Biochem Sci* 22: 383–387, 1997.
53. Winkler BS. Glycolytic and oxidative metabolism in relation to retinal function. *J Gen Physiol* 77: 667–692, 1981.
54. Zeevalk GD and Nicklas WJ. Chemically induced hypoglycemia and anoxia: relationship to glutamate receptor-mediated toxicity in retina. *J Pharmacol Exp Ther* 253: 1285–1292, 1990.
55. Zeevalk GD, Bernard LP, Manzino L, and Sonsalla PK. Differential sensitivity of mesencephalic neurons to inhibition of phosphatase 2A. *J Pharmacol Exp Ther* 298: 925–933, 2001.

Address reprint requests to:
Gail D. Zeevalk, Ph.D.
UMDNJ–Robert Wood Johnson Medical School
Building UBHC, Room 401D
Department of Neurology
675 Hoes Lane
Piscataway, NJ 08854

E-mail: zeevalgd@umdnj.edu

Received for publication March 17, 2004; accepted November 30, 2004.

This article has been cited by:

1. Nian Xiong, Xi Long, Jing Xiong, Min Jia, Chunnuan Chen, Jinsha Huang, Devina Ghoorah, Xiangquan Kong, Zhicheng Lin, Tao Wang. 2012. Mitochondrial complex I inhibitor rotenone-induced toxicity and its potential mechanisms in Parkinson's disease models. *Critical Reviews in Toxicology* **42**:7, 613-632. [CrossRef]
2. Gail D. Zeevalk, Laura P. Bernard, F. T. Guilford. 2010. Liposomal-Glutathione Provides Maintenance of Intracellular Glutathione and Neuroprotection in Mesencephalic Neuronal Cells. *Neurochemical Research* **35**:10, 1575-1587. [CrossRef]
3. Mingchao Liu, Tongjian Cai, Fang Zhao, Gang Zheng, Qiang Wang, Yaoming Chen, Chuanshu Huang, Wenjing Luo, Jingyuan Chen. 2009. Effect of Microglia Activation on Dopaminergic Neuronal Injury Induced by Manganese, and Its Possible Mechanism. *Neurotoxicity Research* **16**:1, 42-49. [CrossRef]
4. Brandi R. Whatley, Lian Li, Lih-Shen Chin. 2008. The ubiquitin–proteasome system in spongiform degenerative disorders. *Biochimica et Biophysica Acta (BBA) - Molecular Basis of Disease* **1782**:12, 700-712. [CrossRef]
5. Ferogh A. Ahmadi, Tom N. Grammatopoulos, Andy M. Poczobutt, Susan M. Jones, Laurence D. Snell, Mita Das, W. Michael Zawada. 2008. Dopamine Selectively Sensitizes Dopaminergic Neurons to Rotenone-Induced Apoptosis. *Neurochemical Research* **33**:5, 886-901. [CrossRef]
6. Myriam Escobar-Khondiker, Damien Toulorge, Serge Guerreiro, Etienne C. Hirsch, Patrick P. MichelDissociated mesencephalic cultures 389-408. [CrossRef]
7. G.D. Zeevalk, L. Manzino, P.K. Sonsalla, L.P. Bernard. 2007. Characterization of intracellular elevation of glutathione (GSH) with glutathione monoethyl ester and GSH in brain and neuronal cultures: Relevance to Parkinson's disease. *Experimental Neurology* **203**:2, 512-520. [CrossRef]
8. Lisa M. Domico, Gail D. Zeevalk, Laura P. Bernard, Keith R. Cooper. 2006. Acute neurotoxic effects of mancozeb and maneb in mesencephalic neuronal cultures are associated with mitochondrial dysfunction. *NeuroToxicology* **27**:5, 816-825. [CrossRef]
9. U. Yazdani, D.C. German, C.-L. Liang, L. Manzino, P.K. Sonsalla, G.D Zeevalk. 2006. Rat model of Parkinson's disease: Chronic central delivery of 1-methyl-4-phenylpyridinium (MPP+). *Experimental Neurology* **200**:1, 172-183. [CrossRef]
10. Marie-Francoise Chesselet, Pierre-Olivier Fernagut, Sheila Fleming. 2005. Parkinson's disease models: From toxins to genes. *Drug Discovery Today: Disease Models* **2**:4, 299-303. [CrossRef]
11. G.D. Zeevalk , L.P. Bernard , C. Song , M. Gluck , J. Ehrhart . 2005. Mitochondrial Inhibition and Oxidative Stress: Reciprocating Players in Neurodegeneration. *Antioxidants & Redox Signaling* **7**:9-10, 1117-1139. [Abstract] [Full Text PDF] [Full Text PDF with Links]
12. Todd B. Sherer , J. Timothy Greenamyre . 2005. Oxidative Damage in Parkinson's Disease. *Antioxidants & Redox Signaling* **7**:5-6, 627-629. [Citation] [Full Text PDF] [Full Text PDF with Links]